

LINEARIZATION OF CMOS LNA'S VIA OPTIMUM GATE BIASING

Vladimir Aparin, Gary Brown

QUALCOMM Inc.
5775 Morehouse Drive
San Diego, CA 92121, USA

Lawrence E. Larson

University of California in San Diego
9500 Gilman Drive
La Jolla, CA 92093, USA

ABSTRACT

A FET linearization technique based on optimum gate biasing is investigated at RF. A novel bias circuit is proposed to generate the gate voltage for zero 3rd-order nonlinearity of the FET transconductance. The measured data show that a peak in IIP_3 occurs at a gate voltage slightly different from the one predicted by the dc theory. The origins of this offset are explained based on a Volterra series analysis and confirmed experimentally. The technique was used in a $0.25\mu\text{m}$ CMOS cellular-band CDMA LNA. At the optimum bias, the amplifier achieved a NF of 1.8dB, an IIP_3 of +10.5dBm, and a power gain of 14.6dB with a current consumption of only 2mA from 2.7V supply.

1. INTRODUCTION

The single-tone desensitization requirement for CDMA phones demands a very high LNA IIP_3 in combination with low NF, high gain and low current consumption. This design challenge requires the use of linearization techniques. A simple technique based on low-frequency low-impedance termination of the LNA input has been shown to work reliably in Si BJT and SiGe HBT LNAs [1]. But it is not applicable to FETs. In [2], feed-forward linearization was used to achieve a very high IIP_3 of a CMOS LNA. Since this technique is very sensitive to mismatches between the main and auxiliary gain stages and errors in the signal scaling, it is rarely used in high-volume production. A FET can also be linearized by biasing at a gate-source voltage (V_{GS}) at which the 3rd-order derivative of its dc transfer characteristic is zero [3]. One of the major drawbacks of this technique is that a significant IIP_3 improvement occurs in a very narrow V_{GS} range (about 10-20mV) around the optimum voltage and there are no known bias means to automatically generate this voltage. Therefore, a bias circuit has to be manually tuned to this voltage, which makes IIP_3 to vary significantly with process and temperature variations.

This paper proposes a novel bias circuit that generates the gate bias voltage at which the 3rd-order nonlinearity of the FET transconductance is zero and automatically tracks

the process and temperature variations. The effect of the optimum gate biasing on linearity at RF frequencies is analyzed using Volterra series. We show that there exist an offset between V_{GS} at which IIP_3 peaks and V_{GS} at which the 3rd-order nonlinearity of the FET transconductance is zero. The origins of this offset are explained. Measured data collected on a $0.25\mu\text{m}$ CMOS LNA designed for cellular CDMA applications confirm the theoretical findings.

2. DC THEORY OF OPTIMUM GATE BIASING

Consider a common-source FET biased in saturation. Its small-signal output current can be expanded into the following power series in terms of the small-signal gate-source voltage v_{gs} around the bias point

$$i_d(v_{gs}) = g_1 v_{gs} + g_2 v_{gs}^2 + g_3 v_{gs}^3 + \dots \quad (1)$$

where g_1 is the small-signal transconductance and the higher-order coefficients (g_2, g_3 etc.) define the strengths of the corresponding nonlinearities. Among these coefficients, g_3 is particularly important because it controls the 3rd-order intermodulation distortion (IM_3) at low signal levels and, thus, determines IIP_3 , which is given by

$$A_{IP3} = \sqrt{\frac{4}{3} \left| \frac{g_1}{g_3} \right|} \quad [\text{V}]. \quad (2)$$

The power series coefficients generally depend on the dc gate-source and drain-source voltages, V_{GS} and V_{DS} . However, the dependence on V_{DS} for a FET in saturation can be neglected. Then the coefficients of (1) can be found as

$$g_1(V_{GS}) = \frac{\partial I_D}{\partial V_{GS}}, \quad (3a)$$

$$g_2(V_{GS}) = \frac{1}{2} \frac{\partial^2 I_D}{\partial V_{GS}^2} = \frac{1}{2} \frac{\partial g_1(V_{GS})}{\partial V_{GS}}, \quad (3b)$$

$$g_3(V_{GS}) = \frac{1}{6} \frac{\partial^3 I_D}{\partial V_{GS}^3} = \frac{1}{3} \frac{\partial g_2(V_{GS})}{\partial V_{GS}}. \quad (3c)$$

As an example, we measured the dc transfer characteristic of a $350\mu\text{m}/0.25\mu\text{m}$ NFET used in the LNA described

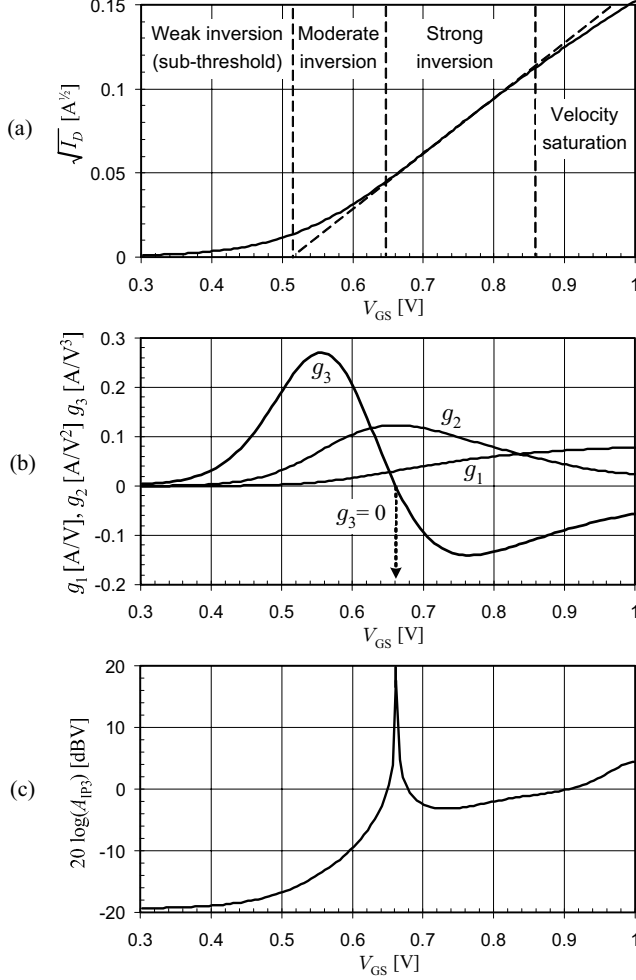


Fig. 1. 350 $\mu\text{m}/0.25\mu\text{m}$ NFET. (a) Measured dc transfer characteristic. (b) Power series coefficients. (c) Theoretical A_{IP3} .

later here. Then, we extracted its power series coefficients and calculated A_{IP3} using (2). The results are presented in Fig. 1. As can be seen, in the transition region from moderate to strong inversion, there is a V_{GS} at which $g_3 = 0$ and $A_{IP3} = \infty$. The peak in A_{IP3} is very narrow and requires an accurate biasing within $\pm 10\text{mV}$ of the optimum voltage. Manually tuned bias circuits are not capable of such precision in the presence of process and temperature variations.

3. BIAS CIRCUIT FOR ZERO G_3

In order for a bias circuit to generate and automatically maintain the bias voltage for zero g_3 , it should produce a dc voltage or current proportional to g_3 and have a dc feedback to set it to zero. The insight into how to design such a bias

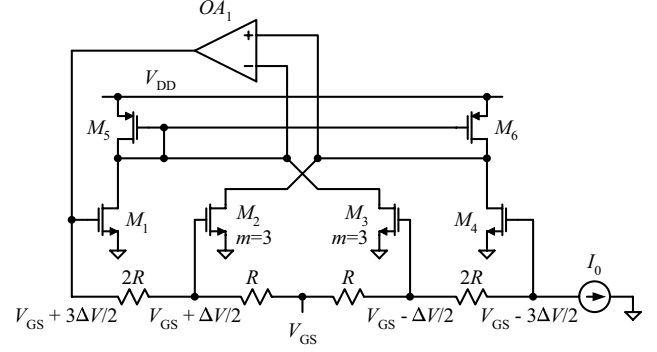


Fig. 2. Bias circuit for zero g_3 .

circuit can be gained if equations (3a)-(3c) are rewritten in terms of small deviations of the dc voltages and currents:

$$g_1(V_{GS}) = \frac{I_D(V_{GS} + \Delta V/2) - I_D(V_{GS} - \Delta V/2)}{\Delta V}, \quad (4a)$$

$$g_2(V_{GS}) = \frac{g_1(V_{GS} + \Delta V/2) - g_1(V_{GS} - \Delta V/2)}{2\Delta V} = \frac{I_D(V_{GS} + \Delta V) + I_D(V_{GS} - \Delta V) - 2I_D(V_{GS})}{2\Delta V^2}, \quad (4b)$$

$$g_3(V_{GS}) = \frac{g_2(V_{GS} + \Delta V/2) - g_2(V_{GS} - \Delta V/2)}{3\Delta V} = \frac{1}{6\Delta V^3} \left[I_D(V_{GS} + 3\Delta V/2) + 3I_D(V_{GS} - \Delta V/2) - 3I_D(V_{GS} + \Delta V/2) - I_D(V_{GS} - 3\Delta V/2) \right]. \quad (4c)$$

If the term in the brackets of (4c) is zero, then $g_3=0$. The bias circuit that generates this term and automatically tunes V_{GS} for zero g_3 is shown in Fig. 2. FETs M_1 - M_4 are scaled versions of the main transistor (not shown). They are built of the same unit cells. M_2 and M_3 have three times more unit cells than M_1 and M_4 . M_1 generates the first current in the brackets of (4c). M_2 generates three times the third current. M_3 generates three times the second current and M_4 generates the fourth current. The currents of M_1 and M_3 (as well as M_2 and M_4) are added by connecting their drains together. The common drains are biased through the current mirror M_5/M_6 where M_5 and M_6 are PFETs of equal size. If the drain voltages of M_5 and M_6 are equal, their currents are equal and the term in the brackets of (4c) is zero. This balance is ensured by the operational amplifier OA_1 that senses the difference between the drain voltages and generates the input voltage for the resistor chain $2R/R/R/2R$ creating a feedback loop. The generated bias voltage for the main FET is tapped at the center of the resistor chain.

The generated V_{GS} is fairly insensitive to the value of ΔV ($=2I_0R$) as indicated in Fig. 3. However, it is very sensitive to mismatches between M_1 - M_4 . Its deviation from the optimum V_{GS} is maximum if the threshold voltage of

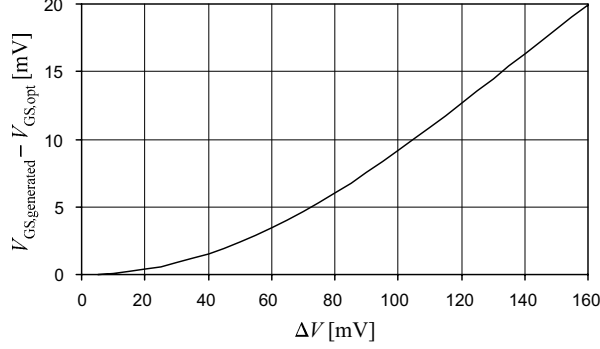


Fig. 3. Simulated deviation of generated V_{GS} in Fig. 2 from the optimum voltage for zero g_3 as a function of ΔV .

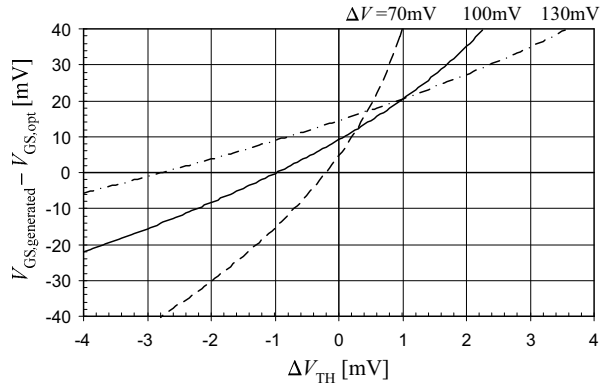


Fig. 4. Simulated deviation of generated V_{GS} from the optimum voltage for zero g_3 as a function of ΔV_{TH} .

M_1 and M_3 shifts in one direction and that of M_2 and M_4 shifts in the opposite direction. For simplicity, we will assume that M_1 is matched to M_3 and M_2 to M_4 . Fig. 4 plots the deviation of the generated V_{GS} from the optimum V_{GS} as a function of the threshold voltage mismatch between M_1/M_3 and M_2/M_4 for different values of ΔV . Positive ΔV_{TH} corresponds to lower V_{TH} of M_1/M_3 than that of M_2/M_4 . As can be seen, a higher threshold of M_1/M_3 compensates for the systematic error in V_{GS} due to ΔV . The standard deviation of ΔV_{TH} can be estimated as [4]

$$\sigma_{\Delta V_{TH}} \approx \frac{A_{V_{TH}}}{\sqrt{W L_g n_f}} \quad [\text{mV}] \quad (5)$$

where $A_{V_{TH}} \approx 1\text{mV}\mu\text{m}$ per 1nm of the gate oxide thickness, W is the gate finger width in μm , L_g is the gate length in μm , and n_f is the total number of gate fingers in M_1 and M_3 (or M_2 and M_4). For the given $0.25\mu\text{m}$ CMOS process, the oxide thickness is 5nm and, thus, $A_{V_{TH}} = 5\text{mV}\mu\text{m}$. With $W = 10\mu\text{m}$, $L_g = 0.25\mu\text{m}$ and $n_f = 20$, we get $\sigma_{\Delta V_{TH}} = 0.71\text{mV}$. As can be seen from Fig. 4, to minimize

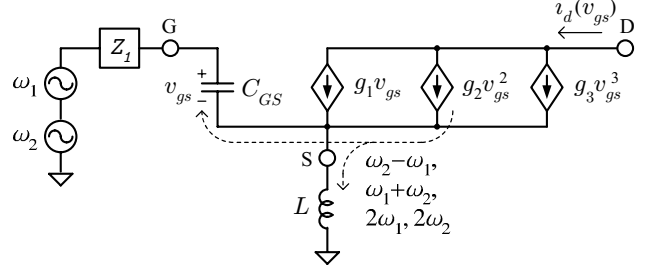


Fig. 5. Small-signal nonlinear equivalent circuit of a common-source FET.

the V_{GS} error within 2-3 times $\sigma_{\Delta V_{TH}}$, ΔV should be more than 100mV. This error is still larger than the V_{GS} range within which a significant IIP_3 improvement occurs (see Fig. 1(c)). To further reduce the V_{GS} error, a process with thinner gate oxide can be selected.

4. RF THEORY OF OPTIMUM GATE BIASING

Consider a small-signal nonlinear equivalent circuit of a FET shown in Fig. 5 where Z_1 is the transformed output impedance of the signal generator and L is the source degeneration inductance. Here we neglect C_{GD} and the nonlinearities of the order higher than three. In this *weakly nonlinear* case, the IM_3 distortion would be generated entirely by the $g_3 v_{gs}^3$ component of the drain current if L was zero. The source degeneration inductance creates a feedback path for the drain current to v_{gs} . This feedback is particularly strong for high frequency spectral components of i_d . For example, the 2nd harmonics generated by $g_2 v_{gs}^2$ are fed back across the gate and source adding to the fundamental components of v_{gs} . These spectral components are then mixed in $g_2 v_{gs}^2$ to produce the responses at $2\omega_1 \pm \omega_2$ and $2\omega_2 \pm \omega_1$. Thus, the 2nd-order nonlinearity of i_d also contributes to IM_3 .

Reusing the Volterra series results for the circuit in Fig. 5 from [1] and assuming that $\Delta\omega (= \omega_2 - \omega_1)$ is much smaller than ω_1 and ω_2 such that $j\Delta\omega L \approx 0$ and the signal generator is conjugately matched to the FET input at ω_1 and ω_2 , we get the following expression for IIP_3 :

$$IIP_3 = \frac{4g_1^2 \omega^2 L C_{GS}}{3|\varepsilon(\Delta\omega, 2\omega)|} \quad (6)$$

where

$$\varepsilon(\Delta\omega, 2\omega) = g_3 - \frac{2g_2^2/(3g_1)}{1 + \frac{1}{j2\omega L g_1} + \frac{j2\omega}{\omega_T} + \frac{Z_1(2\omega)}{\omega_T L}}, \quad (7)$$

$\omega \approx \omega_1 \approx \omega_2$ and $\omega_T = g_1/C_{GS}$. A peak in IIP_3 occurs when g_3 is equal to the real part of the second term in (7). It can be shown that this real part is positive and,

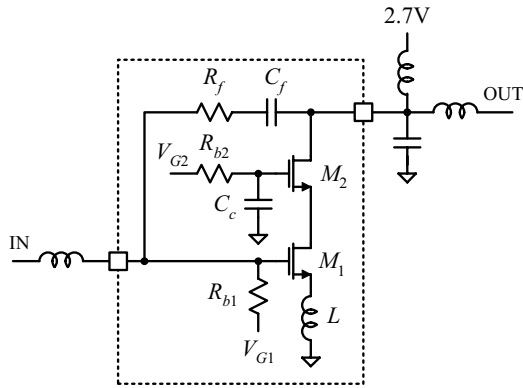


Fig. 6. Simplified schematic diagram of LNA.

therefore, g_3 must be positive as well for the real part of $\varepsilon(\Delta\omega, 2\omega)$ to be zero. As a result, the peak in IIP_3 occurs below the optimum bias voltage for zero g_3 . The imaginary part of $\varepsilon(\Delta\omega, 2\omega)$ limits the magnitude of this peak. For a relatively large degeneration inductance, IIP_3 may not peak at all. We found that the imaginary part of the second term in (7) can be tuned to zero by optimizing the load impedance of the FET drain. However, the real part of this term will remain nonzero causing a shift in the IIP_3 peak.

5. LNA DESIGN AND MEASURED RESULTS

To prove our theory, a cellular-band CDMA LNA was designed and fabricated in $0.25\mu\text{m}$ CMOS technology. Its schematic is shown in Fig. 6 where the dashed box indicates the chip boundaries. The source degeneration inductor is just a bondwire ($\approx 0.45\text{nH}$). The load impedance presented to the drain of M_1 is optimized by tuning C_c such that the imaginary part of (7) is nearly zero. The measured IIP_3 as a function of V_{G1} with two tones centered at 880MHz and separated by 1MHz is shown in Fig. 7 together with g_3 of M_1 . The IIP_3 exhibits a sharp peak of +10.5dBm at a voltage that is 22mV below V_{G1} at which g_3 is zero. The latter gives IIP_3 of only +3.2dBm. To verify that the offset between V_{G1} for peak IIP_3 and V_{G1} for zero g_3 is due to the LNA reactances, IIP_3 of the same LNA was also measured with the two tones centered at 10MHz and its dependence on V_{G1} is plotted in Fig. 7. As can be seen, IIP_3 in this case peaks exactly at V_{G1} at which $g_3=0$. The measured LNA gain and NF are 14.6dB and 1.8dB respectively at the peak- IIP_3 bias in the cellular frequency band. The current consumption is 2mA from 2.7V excluding the bias circuit.

6. CONCLUSIONS

We have shown that biasing a common-source FET at V_{GS} for zero g_3 causes a significant improvement in IIP_3 at

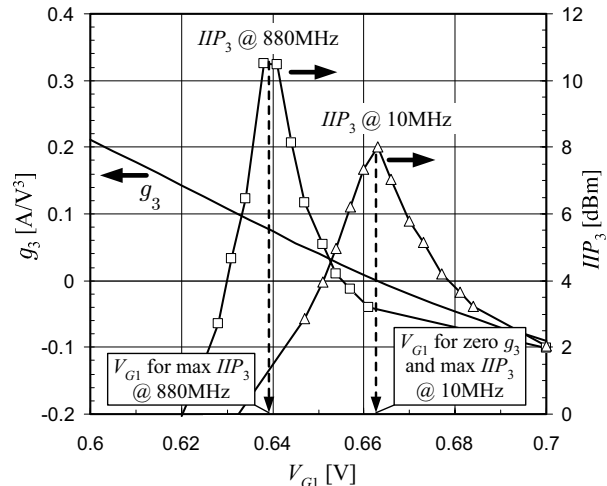


Fig. 7. Measured LNA IIP_3 and extracted g_3 of M_1 as functions of M_1 gate bias.

low frequencies. We proposed a bias circuit that automatically generates this optimum voltage and showed that its precision can be satisfactory, provided that the mismatch between the reference FET's is reduced by increasing their total gate area and selecting a process with a thin gate oxide. We analyzed the effect of the optimum gate biasing on IIP_3 at RF and showed that the circuit reactances that introduce feedback can shift the peak in IIP_3 away from the bias voltage for zero g_3 and reduce the magnitude of this peak. We proposed a method based on tuning the drain load impedance to cancel the effect of the reactances on the maximum IIP_3 . However, the offset between V_{GS} at which IIP_3 is maximum and V_{GS} at which $g_3 = 0$ can not be cancelled. Thus, a manual bias tuning is required to achieve a significant IIP_3 improvement at RF making this technique sensitive to process and temperature variations.

7. REFERENCES

- [1] V. Aparin and L. E. Larson, "Linearization of monolithic LNAs using low-frequency low-impedance input termination," *Europ. Solid-State Circ. Conf.*, pp. 137-140, Sept. 2003.
- [2] Y. Ding and R. Harjani, "A +18dBm IIP_3 LNA in $0.35\mu\text{m}$ CMOS," *IEEE ISSCC*, pp. 162-163, 2001.
- [3] G. Qu and A. E. Parker "Analysis of intermodulation nulling in HEMTs," *Conf. on Optoelectr. & Microelectr. Mat. & Dev.*, pp. 227-230, Dec. 1996.
- [4] M. J. M. Pelgrom, H. P. Tuinhout, and M. Vertregt, "Transistor matching in analog CMOS applications," *IEDM Dig.*, pp. 915-918, Dec. 1998.